B01

Proceedings of the 5th International Conference on Inverse Problems in Engineering: Theory and Practice, Cambridge, UK, 11-15th July 2005

TRANSIENT HEAT TRANSFER FOR CIRCULAR JET IMPACTING A HORIZONTAL SURFACE: APPLICATION OF THE ITERATIVE REGULARIZATION METHOD

J. B. BAONGA, H. LOUAHLIA-GUALOUS, E. ARTIOUKHINE and P. K. PANDAY
FEMTO ST, CREST department, CNRS-UMR 6174, 2 avenue Jean Moulin, 90000 Belfort, France
e-mail: hasna.gualous@utbm.fr

Abstract - This paper presents the experimental results of the local thermal boundary conditions obtained by solving the transient inverse heat conduction problem. The experimental study concerns the heat transfer of a liquid circular jet impinging a horizontal surface. The water is used as the test fluid with the uniform temperature. An electric resistance heater is placed inside the cylinder and 50 thermocouples are installed in order to measure the temperature in the solid. The iterative regularization method is used to solve the transient inverse problem under study. The unknown functions are approximated by cubic B-splines. The gradient is computed by using the adjoint equations.

NOMENCLATURE

f	temperature function, K
h	heat transfer coefficient, W/m^2K
J	residual functional, K^2m
N	angular nodes number
Q	heat flux, W/m^2
r	radius, m
R_2	radius of the heated surface, m
r_n	co-ordinate of measurement point
T	calculated temperature, K
T_{meas}	measured temperature, K
z	axial co-ordinate, m
z_n	co-ordinate of measured point, m

Greek symbols

λ	thermal conductivity, W/mK
θ	temperature variation
Ψ	Lagrange multiplier
γ	descent parameter
δ	Dirac function

Subscripts

n	measured points
w	wall
it	iteration number
r	local value

1. INTRODUCTION

Jet impingement heat transfer has been employed in many practical applications for cooling and drying because it provided high heat transfer coefficient. Jet impingement cooling has been used in a many applications from the metal sheet industry to cooling laser and electronic equipments. Extensive numerical and experimental studies on heat transfer and hydrodynamics of liquid jet impingement have been reported in the literature [1-4]. The applications of liquid jet included cooling in internal combustion engines, quenching of metals and other materials in manufacturing process, and thermal control of high performance computer components.

When a circular liquid jet strikes a flat plate, it spreads radially in very thin film along the heated surface. Following many authors [5,6], the jet impingement flow is divided into four regions defined as: (i) the stagnation zone where the heat transfer is maximal, (ii) the viscous boundary layer zone where the dynamic boundary thickness is lower than the film thickness, (iii) the thermal boundary layer where the film thickness is higher than the thermal boundary layer, (iv) the fully thermal and viscous boundary layer region and (v) the hydraulic jump where the liquid sheet thickness is increased and the jump is associated with a Rayleigh-Taylor instability. Numerous studies are conducted in order to evaluate the average heat transfer coefficients, but the estimation of the transient-state local heat transfer without neglecting the heat conduction in the solid has not retained much

attention. The analysis of thermal performance in the liquid jet impingement requires the knowledge of the thermal boundary conditions for the cooling surface. In this case, the direct measurements of the velocity and temperature distributions in the flowing film are very difficult to carry out because the film thickness is generally less than 500 μm. Only the inlet bulk temperature of the film and the wall temperature inside the experimental cylinder are easily to measure without perturbing the liquid jet flow.

In this work, the procedure for solving the two-dimensional unsteady linear inverse heat conduction problem (IHCP) is presented. It is applied to the problem of the liquid jet impinging the horizontal surface in order to estimate the thermal boundary condition of a hollow half-cylinder. The iterative regularization method is used to solve the inverse problem under analysis. The method is based on the conjugate gradient method that uses to minimize the residual functional and the residual discrepancy principal as the regularizing stopping criterion. This paper presents the results of the experimental study of heat transfer coefficient for a free water jet impacting an horizontal plate. The measured average heat transfer coefficients are compared to the values estimated by solving IHCP.

2. EXPERIMENTAL SET UP

The test facility shown in Figure 1 is composed of two circuits. The first one is a closed circuit where the test liquid is in forced circulation using the pump (13). The fluid in the reservoir (1) is cooled trough the heat exchanger (14). The second circuit consists of the feed to the test section. The fluid is circulated using the pump (2) from the reservoir (1) to the adjustable constant head tank (5) equipped with a drain and an overflow. A filter (3) is used to eliminate any dust or particles in the working fluid. An electrical heater of 250W (7) associated with a temperature system controller (8) are installed in the head tank (5) to control the temperature of the test liquid. A Chromel-Alumel thermocouple (6) is placed in the liquid bath to measure the temperature of the fluid in order to estimate the liquid properties. The fluid from the overhead tank (5) flows under gravity through the regulating valves to the heated surface. The temperature of the working fluid in the reservoir (1) is controlled by using the heater cartridge of 1000W (11) and the regulating system (9).

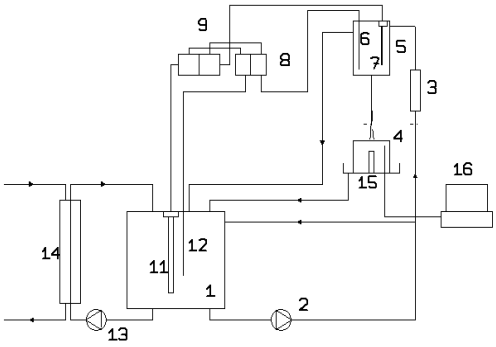

1- reservoir
2- pump
3- filter
4- test section
5- head tank
6- thermocouple
7- heater
8, 9- regulating systems
11- heater
12- thermocouple
13- pump
14- heat exchanger

Figure 1. Experimental apparatus

Figure 2a shows the heater assembly used in this study. The experimental cylinder was made of a brass block and it was heated by using one cartridge heater of 200W. The electric heater has a 10 mm of diameter and 40 mm of length. It is placed inside the experimental cylinder as shown in Figure 1. The electric power input is measured using an ammeter and a voltmeter. The test sample is oriented vertically and is of 50 mm of diameter and 16 mm of length. The cooling circular plane surface is of 50 mm of diameter. The heating cylinder is thermally insulated with Teflon (thermal conduction of 0.23 W/mK) on all faces except the cooling face in order to prevent the heat loss. The test sample can be moved along the vertical axis in order to study the influence of the space between the nozzle and the heated surface. The temperatures inside the experimental cylinder are measured with 50 Chromel-Alumel thermocouples of diameter 0.2 mm (uncertainty of ±0.1°C), placed in two section defined at 0.6 mm and 8 mm from the cooling surface (Figure 2b). For the section S_1, 25 thermocouples are placed at 0.6 mm from the wetted surface at intervals of 3.5 mm°. For the section S_2, 25 thermocouples are used at 8 mm from the outer surface at intervals of 3.5 mm°. The thermocouples are located at 4 concentric circles of radii 8mm, 11.5mm, 15 mm and 22 mm as shown in Figure 2b.

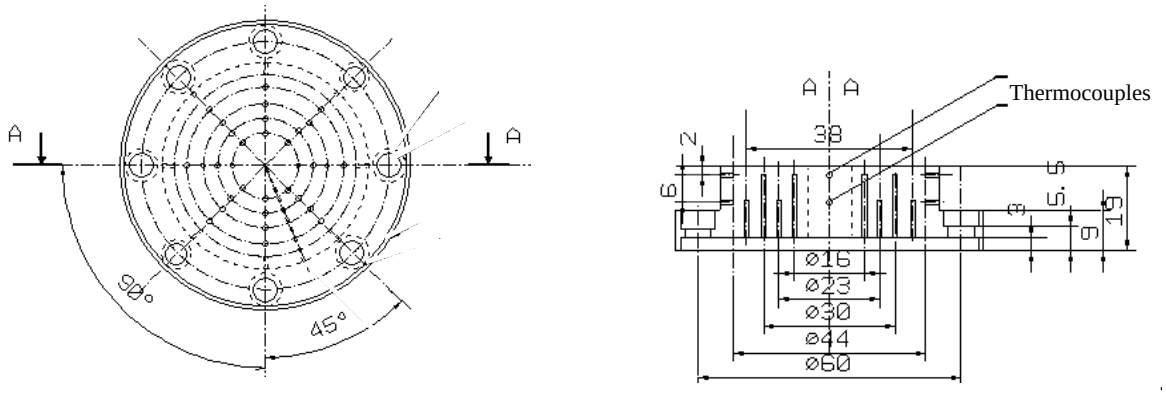

(a) (b)

Figure 2. Instrumentation of the test section.

Because of the uncertainty in the heat flux distribution along the length of the cylinder, the wall temperature distribution was measured at two different sections as shown in Figure 2b. A data acquisition system is used to record all temperature measurements for each imposed electric power inside the experimental cylinder. The IHCP is solved in order to determine the local heat flux and the surface temperature of the heated disk. The local heat transfer coefficient is determined at the exchange circular surface for different flow rates. The experiments are conducted for inlet liquid jet temperature of 37°C, and the total electric power imposed inside the cylinder of 41W and 71W. For each flow rate, the measured temperature inside the wall of the experimental disk is used for solving the IHCP.

3. INVERSE HEAT CONDUCTION PROBLEM

The physical model considers a vertical cylinder of height H and external radius R_2 (Figure 3). The heating cylinder is thermally insulated with Teflon on all faces except the horizontal cooled face in order to prevent the heat loss. The solution of the inverse problem is carried out for half of the cylinder. 50 thermocouples are installed inside the experimental cylinder in order to measure the experimental wall temperature for each test.

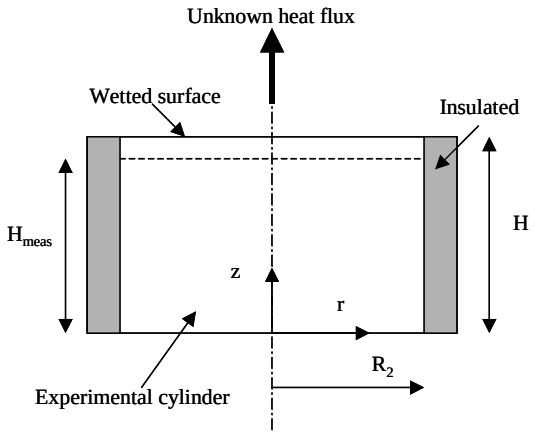

Figure 3. Physical model.

The geometrical and physical properties of the cylinder are presented in Table 1. The mathematical model of a heat conduction process in a hollow cylinder treats the transient-state heat transfer problem. It is given by the following system of equations:

$$\frac{\rho C_p}{\lambda}\frac{\partial T(r,z,t)}{\partial t} = \frac{\partial^2 T(r,z,t)}{\partial r^2} + \frac{1}{r}\frac{\partial T(r,z,t)}{\partial r} + \frac{\partial^2 T(r,z,t)}{\partial z^2}, \text{ where } 0 < r < R_2,\ 0 < z < H \tag{1}$$

$$\frac{\partial T}{\partial r}(0,z,t) = 0, \text{ where } 0 < t \le t_f,\ 0 \le z \le H \tag{2}$$

$$\frac{\partial T}{\partial r}(R_2,z,t) = 0, \text{ where } 0 < t \le t_f,\ 0 \le z \le H \tag{3}$$

$$T(r,z,0) = T_0 \text{ , where : } 0 \le r \le R_2 \text{ , } 0 \le z \le H \tag{4}$$

$$\lambda \frac{\partial T}{\partial z}(r,H,t) = Q_w(r,H,t) \text{ , where : } 0 < t \le t_f \text{ , } 0 \le r \le R_2 \tag{5}$$

$$T(r,0,t) = f(r,t) \text{ , where : } 0 < t \le t_f \text{ , } 0 \le r \le R_2 \tag{6}$$

The mathematical model is supposed symmetrical about the vertical axis of symmetry.

Table 1: Physical properties and geometrical characteristics of the tested cylinder.

Physical properties of brass cylinder:	λ=116W/mK , $C_p = 385$ J.kg^{-1}.K^{-1} , ρ=8522kg.m^{-3}
Physical properties of copper cylinder:	$\lambda = 389$ W / mK , $C_p = 401$ J.kg^{-1}.K^{-1} , ρ=8960kg.m^{-3}
Geometrical dimensions of the brass cylinder:	$R_2 = 25$ mm , $H = 8$ mm , $H_{meas} = 7.4$ mm
Geometrical dimensions of the copper cylinder:	$R_2 = 25$ mm , $H = 10$ mm , H_{meas}=8mm

In the inverse problem, the heat flux $Q_w(r,H,t)$ at the external surface of the cylinder is unknown. The temperatures measured at nodes (r_n, z_n) inside the solid are used as an additional information on the temperature distribution in the cylinder to estimate the function $Q_w(r,H,t)$:

$$T_{meas}(r_n, z_n, t) = f_n \text{ , } n = 1,2,..., N_{meas} \tag{7}$$

The IHCP consists in estimating the function $Q_w(r,H,t)$ using the conditions (1)-(7).

The solution of the inverse problem is based on the minimization of the residual functional defined as:

$$J(Q_w) = \frac{1}{2} \sum_{n=1}^{N_{meas}} \int_0^{t_f} \left[T(r_n, z_n, t; Q_w) - f_n \right]^2 dt \tag{8}$$

where $T(r_n, z_n; Q_w)$ are the temperatures at the sensor locations computed from the direct problem (1)-(6).

Formally, the inverse problem consists in minimizing the residual functional under constrains (1)-(6). The unknown heat flux is approximated in the form of a cubic B-spline as follows:

$$Q_w(r,t) = \sum_{j=1}^{m_t} \sum_{i=1}^{m_r} p_{i,j}\, \phi_i(r)\, \phi_j(t) \tag{9}$$

where m_t x m_r is the number of approximation parameters, p_i are the unknown approximation parameters and ϕ_i are the given basis cubic B-spline. Therefore, the IHCP is reduced to the estimation of a vector of parameters $p = [p_1, p_2, ..., p_m]$. The conjugate gradient method is used in order to minimize the residual functional.

The conjugate gradient algorithm is iterative. At each iteration, the successive improvements of desired parameters are built as follows:

$$p_i^{it+1} = p_i^{it} + \gamma^{it} d_i^{it} \text{ , } i = 1, 2, \ldots, m_t \text{ x } m_r \tag{10}$$

where 'it' is an iteration number. γ^{it} is the descent parameter. d^{it} is the descent direction determined by the following expression :

$$d_i^{it} = -g_i^{it} + \beta^{it} d_i^{it-1} \text{ , } i = 1, 2, \ldots, m_t \text{ x } m_r \tag{11}$$

where the parameter β^{it} is computed as follows:

$$\beta^{it} = \frac{\left\langle g^{it} - g^{it-1} , g^{it} \right\rangle}{\left\| g^{it} \right\|^2} \tag{12}$$

where $\langle\ ,\ \rangle$ is the scalar product, $\|\cdot\|$ is the norm and $\beta^0=0$.

To implement the iterative minimization procedure, the vector g is determined by the following equation:

$$G\ g = J'(p) \tag{13}$$

where G is the Gram's matrix for basis functions.

$$G = \left\{G_{i,j} = \langle \phi_i\ ,\ \phi_j \rangle,\ i,\ j = 1, 2, ..., m\right\} \tag{14}$$

$\langle \phi_i\ ,\ \phi_j \rangle$ is the scalar product in the L_2 space. The Gram's matrix is symmetric and positive. Let J'(p) be the vector gradient of the functional J(p) defined as :

$$J'_i = -\int_0^{t_f}\int_0^{R_2} \psi(r, H, t)\ \phi_i\ dr\ dt\ ,\ i = 1, 2, \ldots, m \tag{15}$$

where ψ is the adjoint problem solution.

3.1 Descent parameter

To compute the descent parameter, the linear approximation of the descent parameter is used [7]:

$$\gamma^{it} = -\frac{\displaystyle\int_0^{t_f}\sum_{n=1}^{N_{meas}}\left[T^{it}(r_n, z_n, t; Q_w) - T_{meas}(r_n, z_n, t)\right]\theta^{it}(r_n, z_n, t; \delta Q_w)\ dt}{\displaystyle\int_0^{t_f}\sum_{n=1}^{N_{meas}}\theta^{it}(r_n, z_n, t; \delta Q_w)^2 dt} \tag{16}$$

where $\theta^{it}(r_n, z_n, t; \delta Q_w)$ is computed from the problem in variations at the *it* iteration by using the variation of the unknown heat flux (δQ_w). $\theta^{it}(r_n, z_n, t; \delta Q_w)$ is defined at the sensor locations (r_n, z_n). δQ_w is approximated from a cubic B-spline as follows:

$$\delta Q_w(r, t) = \sum_{j=1}^{m_t}\sum_{i=1}^{m_r} \delta p_{i,j}\ \phi_i(r)\ \phi_j(t) \tag{17}$$

The problem in variations is defined by the following equations:

$$\frac{\rho C_p}{\lambda}\frac{\partial\theta(r, z, t)}{\partial t} = \frac{\partial^2\theta(r, z, t)}{\partial r^2} + \frac{1}{r}\frac{\partial\theta(r, z, t)}{\partial r} + \frac{\partial^2\theta(r, z, t)}{\partial z^2},\ \text{where}\ 0 \le r \le R_2,\ 0 \le z \le H,\ 0 < t \le t_f \tag{18}$$

$$\frac{\partial\theta}{\partial r}(0, z, t) = 0,\ \text{where}\ 0 < t \le t_f,\ 0 \le z \le H \tag{19}$$

$$\frac{\partial\theta}{\partial r}(R_2, z, t) = 0,\ \text{where}\ 0 < t \le t_f,\ 0 \le z \le H \tag{20}$$

$$\theta(r, z, 0) = 0,\ \text{where}:\ 0 \le r \le R_2,\ 0 \le z \le H \tag{21}$$

$$\lambda\frac{\partial\theta}{\partial z}(r, H, t) = \delta Q_w(r, H, t),\ \text{where}:\ 0 < t \le t_f,\ 0 \le r \le R_2 \tag{22}$$

$$\theta(r, 0, t) = 0,\ \text{where}:\ 0 < t \le t_f,\ 0 \le r \le R_2 \tag{23}$$

3.2 Adjoint problem

The necessary conditions of optimization [7] are defined in the form of an adjoint problem which is represented by the following boundary-value problem:

$$-\frac{\rho C_p}{\lambda}\frac{\partial\psi(r, z, t)}{\partial t} = \frac{\partial^2\psi}{\partial r^2} - \frac{1}{r}\frac{\partial\psi}{\partial r} + \frac{1}{r^2}\psi + \frac{\partial^2\psi}{\partial z^2} + S(r, z, t) \tag{24}$$

where: $S(r, z, t) = -\displaystyle\sum_{n=1}^{N_{meas}}\left\{\delta(r, r_n; z, z_n)\times\left[T(r_n, z_n, t; Q_w) - T_{meas}(r_n, z_n, t)\right]\right\}$

and $0 \le r \le R_2,\ 0 \le z \le H,\ 0 < t \le t_f$

$$\frac{\partial\psi}{\partial r}(0, z, t) = \frac{\psi}{r}(0, z, t),\ \text{where}\ 0 < t \le t_f,\ 0 \le z \le H \tag{25}$$

$$\frac{\partial \psi}{\partial r}(R_2, z, t) = \frac{\psi}{r}(R_2, z, t) \text{ , where } 0 < t \le t_f \text{ , } 0 \le z \le H \tag{26}$$

$$\psi(r, z, t_f) = 0 \text{ , where : } 0 \le r \le R_2 \text{ , } 0 \le z \le H \tag{27}$$

$$\lambda \frac{\partial \psi}{\partial z}(r, H, t) = 0 \text{ , where : } 0 < t \le t_f \text{ , } 0 \le r \le R_2 \tag{28}$$

$$\psi(r,0, t) = 0 \text{ , where : } 0 < t \le t_f \text{ , } 0 \le r \le R_2 \tag{29}$$

The gradient of the residual functional is determined by solving the adjoint problem. The symbol $\delta(r, r_n, z, z_n)$ represents the Dirac function. The direct problem, the adjoint problem and the problem in variations are solved using the control volume method [8] and the implicit fractional-step time scheme proposed by Brian [9].

3.3 Regularization

The inverse problem is ill-posed and the numerical results depends on the fluctuation occurring at the measurements. To obtain a stable solution of the IHCP the iterative regularization method is used by stopping iterations at the optimal value of the residual functional which satisfies the following condition:

$$J(Q_w) \approx \delta^2 \tag{30}$$

where δ^2 is the integrated error of the measured data as follows :

$$\delta^2 = \frac{1}{2}\int_0^{t_f} \sum_{n=1}^{N_{meas}} \sigma^2(r_n, z_n, t)dt \tag{31}$$

$\sigma(r_n, z_n, t)$ is the standard deviation of measurement errors for the temperatures measured at the position (r_n, z_n).

In the absence of the measurement errors, the general stopping criterion is defined as:

$$\left| \frac{Q_w^{it}(r, t) - Q_w^{it-1}(r, t)}{Q_w^{it}(r, t)} \right| \le \varepsilon \tag{32}$$

where the small number ε is used equal to 10^{-4}.

3.4 Algorithm

The inverse heat conduction problem is solved using the following iterative procedure:
The calculations are started by using the parameter β and the unknown heat flux $Q_w(r, H, t)$ equal to zero.

(i) solution of the direct problem,
(ii) calculation of the residual functional,
(iii) solution of the adjoint problem,
(iv) calculation of the components of the functional gradient,
(v) calculation of the parameter β,
(vi) calculation of the component of descent direction,
(vii) solution of the problem in variation to determine the parameter γ,
(viii) the new value of the heat flux density is corrected.
If the convergence criterion is not satisfied the iterative procedure is repeated until the functional is minimized.

4. EXPERIMENTAL DATA PROCESSING

The numerical procedure was validated by using the temperature data obtained from the direct problem to simulate the measured temperatures inside the cylinder. The local heat flux required to solve the direct problem is known and is taken variable spatially and temporally.
For each numerical application, the time step size is choose with respect the delta Fourier number condition based on the sensor depth that is defined by the following equation:

$$\Delta Fo = \frac{\lambda}{\rho C_p} \frac{\Delta t}{(H - H_{meas})^2} \ge 0.001 \tag{33}$$

4.1 Numerical verification of the solution procedure

We consider a copper vertical cylinder having 50 mm of diameter and 10 mm of length. We have choose to verify the numerical procedure by using a known heat flux varying with the time and the radius of the cylinder. The heat flux is imposed at the wetted surface of the cylinder (z=H) as shown in Figure 4 by the continuous curve. The downward surface (z=0) is assumed to be isotherm (T(r,0,t)= 40°C). The unknown transient heat flux is assumed to vary as follows:

$$Q_w(r,t)=0.1\left(0.04r^5+184852\,r^4-1161463\,r^3+256664\,r^2+4925260\,r-9996144\right)\left(1+0.01t\right) \quad (34)$$

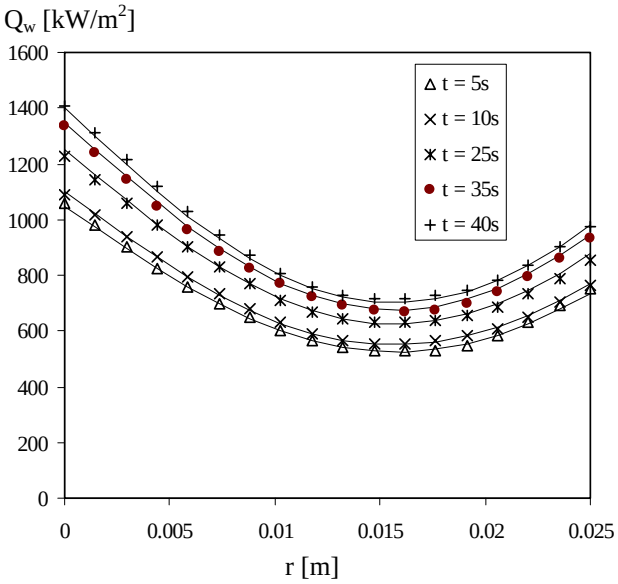

Figure 4. Comparison of the calculated and exact heat fluxes.

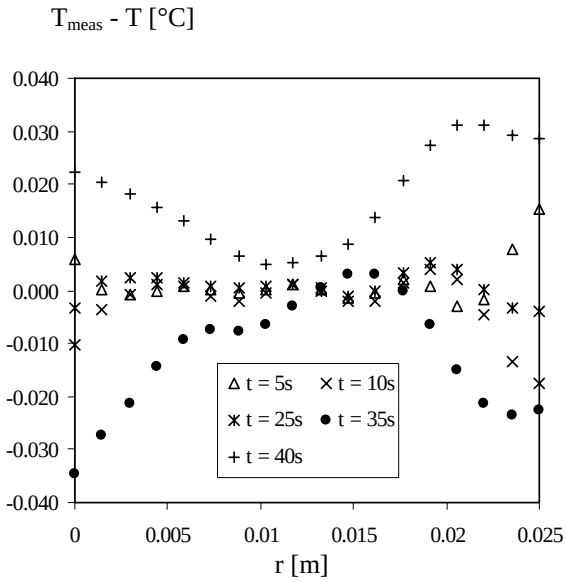

Figure 5. Radial distributions of the temperature residuals.

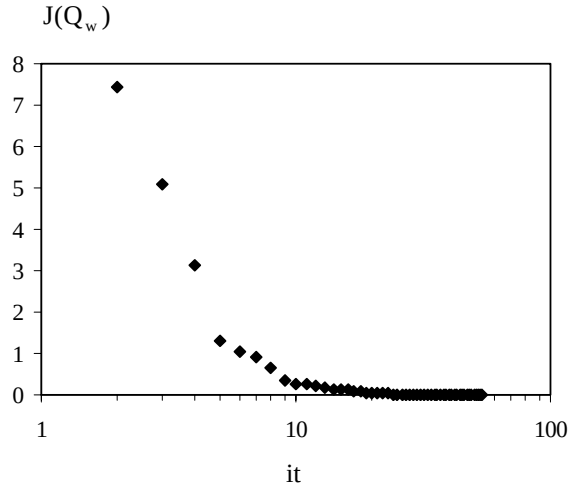

Figure 6. Evolution of residual functional as a function of the number of iterations.

In order to validate the inverse estimation procedure, we have assumed that the temperatures calculated from the direct problem solution at the measurement points are the measured temperatures ($T_{meas}(r_n, z_n, t) = f_n(r_n, z_n, t)$) for solving ICHP. Figure 4 shows that the estimated heat flux practically coincides with the exact heat flux for different times. This validation is carried out for the number of approximation parameters equal to 9x9. Figure 5 shows the difference between the computed temperatures and the simulated measured temperatures. The maximum deviation is of ±0.03°C. Figure 6 shows the evolution of the residual functional $J(Q_w)$ as a function of the number of iterations. The iterations are continued till the convergence criteria $J<10^{-10}$ is satisfied.

4.2 Experimental determination of the local thermal boundary conditions

A vertical brass cylinder having 50 mm of diameter is considered. The sensors locations are showed in Figures 2a and 2b. A grid of 21 nodes along the height of the cylinder and 21 nodes in the radial direction have been used. The local thermal characteristics are computed by solving IHCP where the temperatures measured at downward surface are used as the boundary condition to solve the direct problem. The temperatures measured at

height z = 7.4 mm are used to solve the inverse problem. The computation is conducted by using the number of measurement points equal to the nodes number.

During experiments, the fixed flow rate for the study is first adjusted under gravity using the regulating valves. Initially the cylinder disk is covered in order to prevent the liquid to wet the exchange surface. For a fixed total heat flux, the experimental disk is heated. When the measured wall temperature reached a steady-state, the exchange surface is rapidly uncovered. The liquid jet then hits the heat transfer surface perpendicularly. The time-dependent local wall temperatures is recorded, until the experimental disk reached a new steady-state.

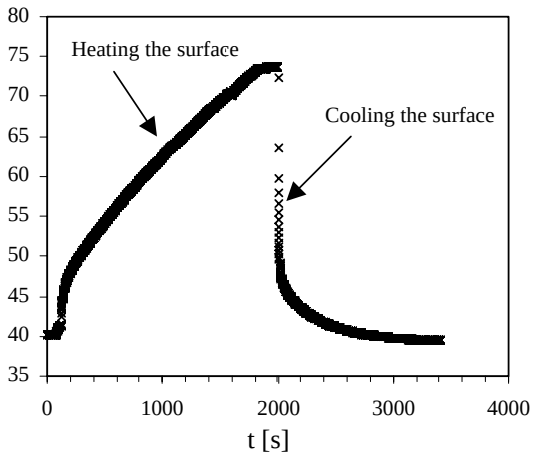

Figure 7. Measured temperature inside the solid.

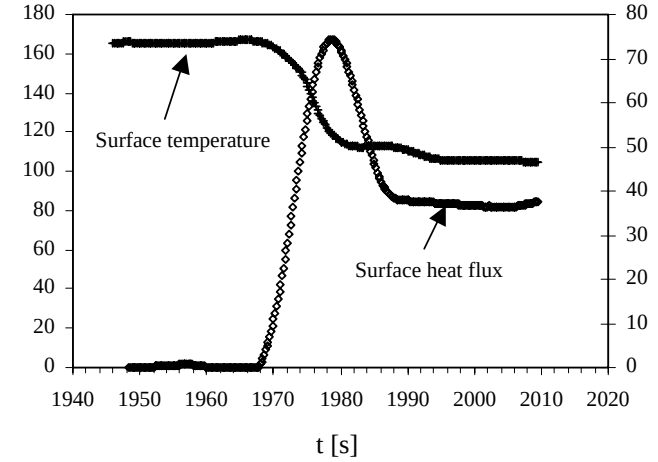

Figure 8. Estimated heat flux and surface temperature.

Figure 7 shows the evolution of the measured temperature inside the solid by the sensor placed in the vertical axis at 0.6mm far from the exchange surface. It shows two different zones, the first one where the surface is not wetted by the water jet and the wall temperature increased continually along the time. The steady state is attained for t approximately equal to 1800s (see Figure 7). After this time, the temperature inside the solid becomes uniform along the time. Figure 7 shows a second zone where the wall temperature decreased along the time because of the jet impacting the heated surface is at the temperature (= 37°C) lower than the wall temperature. When the water jet impacted the heated surface, the wall temperature decreased and attained the stable value during a quick period (20s approximately) from 73.6°C to 39.4°C.

Figure 8 shows the estimation of the surface temperature and the surface heat flux in the stagnation point (r=0) for the phase of the cooling surface. The heat transfer is highest in the zone of the stagnation and the impingement liquid flow situated at the center of the heated surface where the film thickness does approach infinity. After this zone, the heat transfer decreases because the thin film becomes relatively uniform on the wetted surface. Figures 9 and 10 are obtained for the electric power input of 41 W and 71W; and, the flow rate of water jet of 9 g.s^{-1}. The estimated standard deviation of temperature residuals of this computation is of 0.04°C. It is showed that when the jet of the water impacted the heated surface, the dissipated heat flux increased during 12s, decreased during 8s, and finally reached an asymptotic value at the steady state. In this zone, the surface temperature reaches the minimum and it becomes uniform along the time.

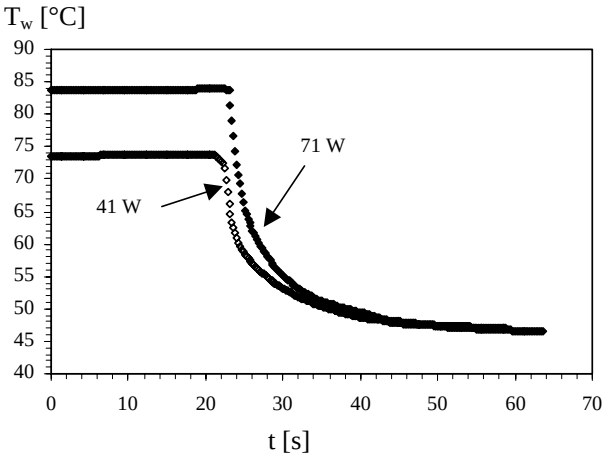

Figure 9. Measured temperature inside the solid.

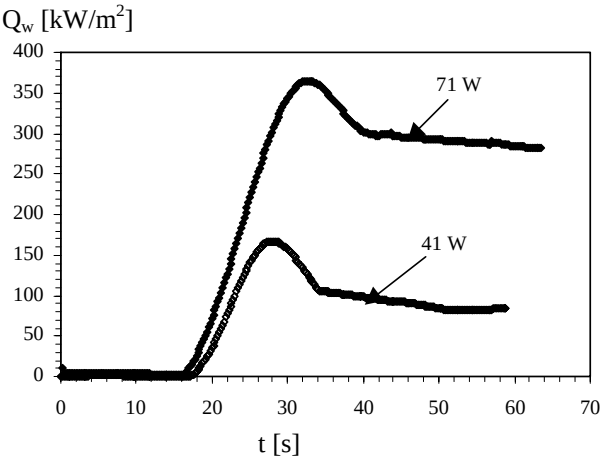

Figure 10. Estimated heat flux.

Figures 9 and 10 show the influence of the electric power imposed inside the solid. For these figures, experiments are conducted for the water inlet temperature of 37°C. For the total electric power of 41W and 71W, Figure 9 shows the measured wall temperature obtained from the thermocouples located in the axial direction at 0.6mm far from the surface. It can be seen that the wall temperature decreased for each electric power and reached the same temperature value at the steady state. Figure 10 shows the distribution of the heat flux after the water jet impacting the heated surface. For 41 W, the heat flux dissipated at the surface reached the new steady state during a time lower than for 71W.

Figure 11 shows the radial distribution of the local Nusselt number for two fixed flow rate of the impinging jet (15 g/s and 4.4 g/s). In this experiment, the power input is of 51W and the inlet temperature of the water (T_i) is of 41°C.

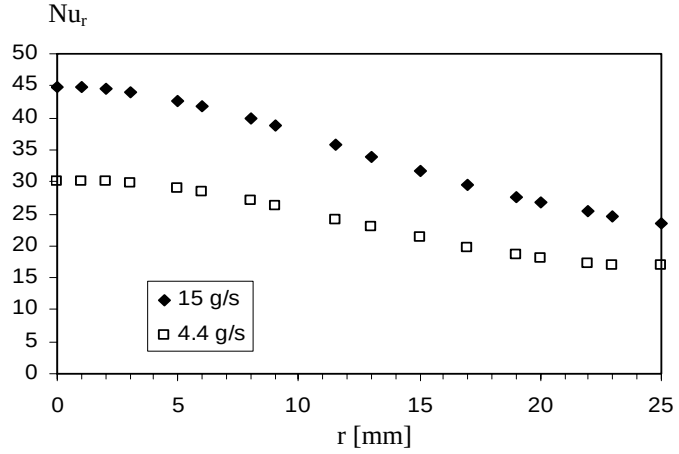

Figure 11. Radial distribution of the local Nusselt number.

The local thermal characteristics are computed by solving the IHCP where the temperatures measured at z=0 are used as the boundary condition to solve the direct problem. The temperatures measured at z=7.4mm are used to solve the inverse problem. The local heat transfer coefficient is calculated from the surface heat flux density ($Q_{w,r}$), the local surface temperature ($T_{s,r}$) as follows:

$$h_r = \frac{Q_{w,r}}{T_{s,r} - T_i} \tag{35}$$

The local Nusselt number is deduced from h_r as:

$$Nu_r = \frac{h_r D}{\lambda} \tag{36}$$

where D is the diameter of the heated surface, λ is the thermal conductivity.

Figure 11 shows that the radial Nusselt number increases with the impinging water flow rate because at higher flow rate the liquid film carries more energy from the heated surface. It is noted that the heat transfer is highest in the stagnation zone where the film thickness does approach infinity. After this zone, the heat transfer decreases in the thin liquid film thickness.

5. CONCLUSIONS

A transient measurement procedure was developed to combine measurements of temperature, IHCP method with jet characteristics and electric power input. This article presents the results obtained by solving the IHCP applied to the cylindrical geometry. The local heat flux and the surface temperature are determined by using the measured temperatures inside the heated solid. This article shows the advantage of using IHCP to determine the thermal boundary characteristics. In this work, the inverse analysis is applied to a particular case of jet impacting the heated surface. In this case, the measurement of the local heat flux or surface temperature is very difficult without perturbing the flow. In more, the comparison of the calculated and exact heat flux and the evolution of calculated and measured temperature show the precise character of the method.

REFERENCES

1. B. Elison and B.W. Webb, Local heat transfer to impinging liquid jets in the initially laminar, transitional, and turbulent regimes. *Int. J. Heat Mass Transfer* (1994) **37**, 1207-1216.

2. Y. Pan and B.W. Webb, Heat transfer characteristics of array of free-surface liquid jets. *Trans. ASME, J. Heat Transfer* (1995) **117**, 878-883.

3. L.M. Jiji and Z.Dagan, Experimental investigation of single-phase multijet impingement cooling of an array of microelectronic heat sources, Cooling Technology for Electronic Equipment. *International Symposium Honolulu,* HA, 1988, pp. 333-351.

4. Y. Pan and B.W. Webb, Visualization of local heat transfer under arrays of free surface liquid jets. *Institution of Chemical Engineers Symposium Series* (1994) **135**, 77-82.

5. E.J. Watson, The radial spread of a liquid over horizontal plane. *J. Fluid Mech*. (1964) **20**, 481-499.

6. X. Liu and J.H. Lienhard V, Liquid impingement heat transfer on a uniform flux surface, *National Heat Transfer Conference*, 1989, pp. 523-530.

7. O.M. Alifanov, E.A. Artyukhin and S.V. Rumyantsev, *Extreme Methods for Solving Ill-Posed Problems with Applications to Inverse Heat Transfer Problems,* Begell House, New York, 1995.

8. S.V. Patankar, *Numerical Heat Transfer and Fluid Flow,* Mc-Graw Hill, New York, 1980.

9. P.L.T. Brian, A finite-difference method of higher order accuracy for solution of three dimensional transient heat conduction. *A.I.Ch.E. J.* (1961) **7**, 367-370.